Effect of a Single Water Molecule on the Electronic Absorption by *o*- and *p*-Nitrophenolate: A Shift to the Red or to the Blue?

Jørgen Houmøller,[a] *Marius Wanko,*[b] *Angel Rubio,*[b,c,]* *and Steen Brøndsted Nielsen*[a,]*

[a] Department of Physics and Astronomy, Aarhus University, DK-8000 Aarhus C, Denmark. [b] Nano-Bio Spectroscopy Group and ETSF, Dpto. Fisica de Materiales, Universidad del País Vasco, CFM CSIC-UPV/EHU-MPC & DIPC, 20018 San Sebastián, Spain. [c] Max Planck Institute for the Structure and Dynamics of Matter and Center for Free-Electron Laser Science, Luruper Chaussee 149, 22761 Hamburg, Germany.

.

KEYWORDS Gas-phase spectroscopy. Microhydration. Charge-transfer excitation. Mass spectrometry. Nitrophenolate. Coupled-cluster calculations.

ABSTRACT Many photoactive biomolecules are anions and exhibit ππ* optical transitions but with a degree of charge transfer (CT) character determined by the local environment. The phenolate moiety is a common structural motif among biochromophores/luminophores, and nitrophenolates are good model systems as the nitro substituent allows for CT-like transitions.

Here we report gas-phase absorption spectra of *o*- and *p*-nitrophenolate·H_2O complexes to decipher the effect of just one H_2O and compare them with ab initio calculations of vertical excitation energies. The experimental band maximum is at 3.01 and 3.00 eV for *ortho* and *para* and is redshifted by 0.13 and 0.10 eV relative to the bare ions. These shifts indicate that the transition has become more CT-like due to localization of negative charge on the phenolate oxygen, *i.e.*, diminished delocalization of the negative excess charge. Still the transition bears less CT than that of *m*-nitrophenolate·H_2O as this complex absorbs further to the red (2.56 eV). Our work emphasizes the importance of local perturbations: One water causes a larger shift than experienced in bulk for *para* and almost the full shift for *ortho*. Predicting microenvironmental effects in the boundary between CT and non-CT with high accuracy is nontrivial. However, in agreement with experiment our calculations show a competition between the effects of electronic delocalization and electrostatic interaction with the solvent molecule. As a result, the excitation energy of *ortho* and *para* is less sensitive to hydration than that of *meta* as donor and acceptor orbitals are only weakly coupled in *meta*.

Introduction

In freshman chemistry courses students are taught that an increase in electron delocalization within a molecule results in a lower gap between the highest-occupied molecular orbital (HOMO) and the lowest-unoccupied molecular orbital (LUMO); this is directly evident from molecular orbital diagrams or the simple electron-in-a-box model with increasing box lengths. These models nicely explain why the absorption band redshifts in the series ethylene, 1,3-butadiene, 1,3,5-hexatriene, etc. However, it is not always this simple: While the absorption by

neutral polycyclic aromatic hydrocarbons (PAHs) duly redshifts with molecular size, a similar trend is not seen for the protonated linear analogues since those with an even number of aromatic rings display pronounced charge-transfer (CT) character (and therefore absorb further to the red than their size justifies) as beautifully demonstrated by Jouvet and co-workers.[1] Likewise, a decrease in delocalization due to for example microsolvation may actually lead to a lower excitation energy (redshifted absorption band) if the electronic transition changes character and becomes CT-like (Figure 1).[2] Hence a description of HOMO-LUMO gaps based alone on electron delocalization is insufficient, and qualitative reasoning is difficult as different effects can shift gap energies in opposite directions with unknown relative importance. Another issue to consider in the case of protonated species is internal proton transfer to the solvent molecules in the ground state when the solvent cluster is large enough.[3,4] Altogether, it implies that it is in general non-trivial to predict the effect of microsolvation or other perturbations on transition energies.

<Please inset Figure 1 here>

The effect of a nearby environment is of particular importance for biochromophores located within protein pockets where there are a limited number of interactions with water molecules or amino acid residues: Examples include the chromophores of the green fluorescent protein (GFP) and the photoactive yellow protein (PYP),[5-13] and the oxyluciferin luminophore located within the luciferase enzyme and responsible for light emission from fireflies;[14-16] the phenolate moiety is a common structural motif for all three in their anionic forms.

As simple model systems for photoactive biomolecules we have studied *o*-, *m*-, and *p*-nitrophenolate isolated *in vacuo* using specialized mass spectroscopy equipment built in Aarhus.[17] The HOMO and the LUMO are delocalized over the whole molecular anion in the former and latter cases (Figure 1) while the *meta* isomer displays CT-like excitation. This conclusion was reached from the *meta* isomer absorbing to the red of *ortho* (***o***) and *para* (***p***) isomers despite a lower electron delocalization (a resonance form where the electron is moved from the phenolate oxygen to the nitrogen group is not allowed in the ground state for *meta*); the redshift is 0.77 eV and 0.81 eV compared to *ortho* and *para* isomers, respectively. We also established that a single water molecule attached to the *meta* phenolate oxygen blueshifts the absorption by 0.22 eV, because upon excitation, the interaction between the water dipole and the center of excess charge is weakened as the latter moves from the phenolate towards the nitro group, i.e., away from the water.[18]

Now a compelling problem that remains to be resolved is whether a single water molecule attached to either ***o*** or ***p*** causes a redshift or a blueshift in the absorption. The water localizes the negative charge at the phenolate oxygen and thereby diminishes the importance of the Lewis resonance structure that assigns the negative charge to the nitro group (Figure 1). *Ortho* and *para* becomes *meta*-like so to speak, that is, decoupling is similar to the situation occurring naturally in the *meta* form, and a single water molecule should therefore give a redshift in the absorption, by as much as 0.8 eV (difference between bare *ortho/para* and bare *meta*). However, the price of moving the electron away from the phenolate oxygen and towards the nitro group also has to be paid, and based on results for the *meta* isomer, this electrostatic effect could be as much as 0.2 eV. Hence we have two opposing effects on the transition energies, and the actual shift from the bare ion absorption is expected to be between –0.8 eV and +0.2 eV.

Here we address the effect of a single water molecule based on gas-phase ion spectroscopy of complexes between *o*- and *p*-nitrophenolate and water and theoretical calculations of excited states.

Experimental section

It is difficult to measure the absorption spectrum of ions *in vacuo* due to a too low ion density for traditional light transmission experiments. Instead the occurrence of light absorption is monitored from ion dissociation (action spectroscopy). The yield of fragment ions as a function of the wavelength of absorbed light is taken to represent the absorption spectrum under the assumption that photoexcitation leads to complete dissociation for all excitation energies within the time window of the experiment, and that the quantum yield for light emission is independent of excitation energy. The former is most easily fulfilled for weakly bound complexes as those under study in this work.

The experimental setup (Figure 2) has been explained in detail elsewhere.[19,20] Briefly, ions were produced by electrospray ionization and subsequently trapped in an octopole for up to 25 ms by pulsing a lens directly after the octopole. Residual gas collisions cooled the ions to approximately room temperature. Water vapor was let into the octopole region to a pressure of 0.01 mbar to 0.1 mbar to form ion-water complexes. All ions were then accelerated to a kinetic energy of 50 keV, and those of interest were selected according to their mass-to-charge ratio by an electromagnet. These then travelled along a straight section where they interacted with a nanosecond-light pulse from a pulsed laser. Photoexcitation led to dissociation that was monitored by a hemispherical electrostatic analyzer (kinetic energy per charge selector). The

yield of the selected fragment ion was counted by a channeltron detector. The time window for fragmentation is a few microseconds.

<Please inset Figure 2 here>

The results shown in this paper are combined measurements from two different wavelength regions. The main laser used is an EKSPLA Q-switched nanosecond pulsed laser, where the third harmonic of a Nd:YAG fundamental is used to pump an optical parametric oscillator (OPO). The output range of the OPO is 420 nm to 2300 nm. To produce light below 420 nm, we constructed a sum-frequency generator (Figure 2). This setup utilizes sum-frequency generation between the Nd:YAG IR fundamental (1064 nm) and the visible light from the OPO, both originating from the same laser. The linear polarization of the visible light is changed by $\pi/2$ from passing through a half-wave plate to allow type-I phase matching in a barium borate (BBO) crystal. A Pellin-Broca prism is used for separation of the IR fundamental, the OPO light, and the sum-frequency light. Angle tuning of the BBO and the prism is achieved by two stepper-motor-rotation stages controlled by a LabView program. The output range of the sum-frequency generation is 301 nm to 425 nm. The output powers of the OPO and the sum-frequency setup are shown in Figure 3.

<Please inset Figure 3 here>

The repetition rate of the ion trap and the laser was 40 Hz and 20 Hz, respectively. Hence after each laser shot, we monitored the background dissociation due to residual gas collisions or unimolecular decay of metastable ions. This ‘laser-off’ signal is proportional to the ion-beam

current, but was too low in these experiments to correct for fluctuations in ion current. Instead the experiment was repeated a number of times to average out any such fluctuations. The 'laser-off' signal was subtracted from the 'laser-on' signal, and the resultant signal was corrected for the number of photons in the laser pulse.

Computational details

If not indicated otherwise, geometries were optimized with the PBE0 functional and aug-cc-pVDZ basis set using the turbomole software.[21] Vertical excitation energies (*VEE*s) were obtained with the CC2 coupled-cluster method[22], its spin-component-scaled version SCS-CC2, the 2nd-order algebraic diagrammatic construction method ADC(2)[23] (turbomole), SORCI[24], and NEVPT2[25] (orca,[26]). For the latter two methods, a CASSCF(12,10) reference was used, which includes the entire π-system. The SORCI calculations start with the CASSCF orbitals and a MRDDCI2 step (thresholds $T_{pre}=10^{-3}$, $T_{sel}=10^{-6}$) to produce approximate 2-state averaged natural orbitals for the final MRDDCI3 calculation. All excited-state calculations were performed with the aug-cc-pVDZ basis. The models for bulk solution contained seven explicit water molecules, forming H-bonds with the solute, and the COSMO solvation model. The ADC(2)+COSMO excitation energies were calculated self-consistently using the cc2cosmo script and including off-diagonal contributions. Binding energies were calculated with CCSD(T) and the aug-cc-pVTZ basis, on SCS-MP2/aug-cc-pVDZ geometries and corrected for BSSE (same level of theory) and ZPVE (from PBE0/aug-cc-pVTZ). Vertical detachment energies were calculated with CCSD(T), like in ref 17. Geometries and further results are provided in the Supporting Information.

Results and discussion

Photodissociation of the ***o***·H_2O and ***p***·H_2O complexes results in only one dominant fragment for each complex corresponding to loss of water (fragment ion *m/z* = 138, see SI). The fragment ion yield increased linearly with laser power (see SI), which indicates that dissociation is due to one-photon absorption, and therefore that the binding energy of the complex is less than the photon energy (>2.5eV). For ***p***·H_2O, we calculated binding energies of 0.41 eV (H-bond to phenolate) and 0.32 eV (H-bond to nitro group) (Figure 4). At room temperature, we therefore expect the first isomer to strongly prevail in the ion beam (assuming that the limiting barrier for moving the water from one end to the other is low enough to allow for equilibrium to establish). Interestingly, the binding energy is lower than that previmetously calculated for the *meta* isomer (0.64 eV)[8], which indicates that some of the negative charge in *para* is still on the nitro group (the donor and acceptor orbitals are not fully decoupled). This is in agreement with absorption spectra to be discussed later. For ***o***·H_2O the water binds to both groups but forms the stronger bond to the phenolate (Figure 4). Assuming that there is no barrier for the reverse reaction, the excess energy after photoexcitation is more than 2 eV (photon energy minus dissociation energy), and it is therefore reasonable to assume that the dissociation of the photoexcited ions occurs within the time window of the experiment (a few μs).

<Please inset Figure 4 here>

Action spectra of the complexes are shown in Figure 5. These were obtained as 'laser on' signal minus 'laser off' signal followed by a linear correction for the number of photons at each wavelength. The band maximum is at 3.01 eV (412 nm) for ***o***·H_2O (Figure 5a) and at 3.00 eV (413 nm) for ***p***·H_2O (Figure 5b).

<Please inset Figure 5 here>

It is evident that the water complexes absorb further to the red than the bare chromophores. The redshift for the *para* isomer [0.13 eV (17 nm)] is greater than that for the *ortho* isomer [0.10 eV (13 nm)]. The fact that a redshift is seen can be explained by the lesser degree of coupling between the donor and acceptor orbitals in the complexes. Judged by the calculated ground-state geometries (Figure 4), it is clear that the overall perturbing effect of the water molecule for the *ortho* isomer must be less than that for the *para* case as both the donor and acceptor groups are in close proximity to the water; this is in accordance with the measured redshifts.

For $\boldsymbol{o}\cdot H_2O$ and $\boldsymbol{p}\cdot H_2O$, we calculated vertical detachment energies of 3.75 eV and 3.83 eV, respectively, which is ca. 0.5 eV higher than those reported for the bare anions[7]. Importantly, these detachment energies are well above the absorption band maxima by more than 0.7 eV, and electron detachment is therefore not expected to be an important channel close to the band maxima.

In aqueous solution, the absorption band maxima of ***o*** and ***p*** are at 3.00 eV (415 nm, Figure 5a) and 3.11 eV (399 nm, Figure 5b), respectively. Interestingly, for ***p*** the shift by one single water molecule is larger than that after full hydration. Indeed the absorption by the bare ion and $\boldsymbol{p}_{(aq)}$ is very similar; full hydration only redshifts the band by 0.03 eV (4 nm). This can easily be rationalized: In the fully hydrated ion, there are water molecules both at the phenolate oxygen and the nitro group, and the donor and acceptor orbitals are therefore coupled, like they are in the bare ion. Interestingly, for the *ortho* isomer, the shift corresponding to bulk solution can be ascribed mainly to the effect from binding a single water molecule.

Furthermore, fully hydrated ***o*** absorbs to the red of $\boldsymbol{p}_{(aq)}$. A polarization effect can account for this: In general, an excited state is more polarizable than a ground state, and movement of electron density towards the water dipoles would bring down the excited state energy of $\boldsymbol{o}_{(aq)}$ (the dipoles at the phenolate oxygen and the nitrogen group point in similar direction). A movement of electron density in the *para* isomer would be beneficial for some water molecules but not for others; the water dipole moments are pointing in different directions at the phenolate oxygen end and the nitro group end.

In order to see if theory can account for the observed hydration effects, we performed a series of quantum chemical calculations at various levels of theory. Based on the minimum-energy geometries, representing the anions and their microhydrated complexes at the 0-K limit (Figure 4), we calculated *VEE*s with the CC2, ADC(2), SORCI, and NEVPT2 methods (summarized in Table 1). The first three methods provide excitation energies that maximally differ by 0.25 eV compared to experimental values while the deviation is as much as 0.5 eV for NEVPT2. All methods consistently predict a small blueshift of both complexes compared to the solute *in vacuo*. Nevertheless, this shift is much smaller than that earlier reported for *meta*: 0.05 eV for *ortho*, 0.24 eV for *meta*, and 0.06 eV for *para* (CC2 method). Hence theory is in accordance with a decoupling of donor and acceptor orbitals in *ortho* and *para* isomers upon water attachment accounting for a smaller shift than seen for the *meta* isomer. The relative importance between decoupling (giving a redshift) and loss of complex binding energy upon photoexcitation (electrostatic effect giving a blueshift) is, however, not correctly predicted.

Krylov and co-workers[12] earlier reported on the effect of attachment of a single water molecule to the isolated chromophore anions of GFP and PYP proteins. They used as model systems deprotonated 4-hydroxybenzylidene-2,3-dimethylimidazolinone (HBDI) and deprotonated *para*-

coumaric acid (pCA) to represent the chromophores in GFP and PYP, respectively. SOS-CIS(D)/cc-pVTZ-calculated *VEE*s for the HBDI anion and EOM-EE-CCSD/6-31+G(d,p) ones for the pCA anion revealed a small blueshift of 0.03 eV and 0.06 eV, respectively, due to the water (in both cases phenolate form of chromophore). These shifts are similar to what we calculate for ***o*** and ***p***.

We also modelled the fully hydrated solute (see Computational Details). Full hydration yields a redshift relative to the bare ion, which varies with the quantum chemistry method, but in all cases is larger for ***p*** than for ***o*** (Table 1). As seen experimentally, theory predicts the absorption by $\boldsymbol{o}_{(aq)}$ to be to the red of $\boldsymbol{p}_{(aq)}$.

In order to investigate how the microhydration affects the CT character and energetics of the excitation, we consider the individual components of the solvent shift, *i.e.*, (1) the change of the solute geometry, (2) the electrostatic interaction energy between the solvent and the polarized solute (V^{ES}), and (3) the electronic reorganization energy invested to polarize the solute (E^{ERO}). The geometry of the solute changes upon binding a water molecule due to the localization of the excess charge on the H-bond accepting group (Table 2). When the water in $\boldsymbol{p}\cdot H_2O$ binds to the phenolate oxygen, the C-O and C-N bonds are stretched by 0.012 and 0.009 Å, respectively, which indicates that the first of the two resonance structures shown in Figure 1 gains weight. The excitation calculated for the bare solute with this displaced geometry shows a slightly increased charge transfer, as measured by the difference in dipole moment (last column in Table 2), but the expected redshift amounts to merely 0.01 eV. The opposite applies when the water binds to the nitro group. The difference in dipole moments is reduced and we obtain a blueshift of 0.03 eV.

In order to calculate the exact contributions of (2) and (3), we replace the water molecule by a set of point charges, as used in the TIP3P water model. This neglects the potential effect of

charge transfer between solute and solvent, but allows us to calculate V^{ES} exactly, based on the relaxed CC2 ground- and excited-state densities. If the water binds to the phenolate group, V^{ES} contributes a blueshift of 0.07 eV, whereas E^{ERO} is nearly the same for ground and excited state, contributing only -0.01 eV to the solvent shift. With the water binding to the nitro group, we obtain -0.03 and -0.01 eV for V^{ES} and E^{ERO}, respectively. An alternative decomposition that considers the polarization energy (Supporting Information, Table S2) yields the same trend. In summary, our calculations confirm a decoupling of donor and acceptor states in the $\boldsymbol{p}\cdot H_2O$ complex, but the predicted effect on the absorption energy is rather small and overcompensated by the electrostatic interaction. The same trends were obtained with CC2 using PBE0 geometries (Table S1, Supporting Information).

Conclusions

In conclusion, we have shown that a single water molecule attached to *o*- and *p*-nitrophenolate perturbs the electronic structure to produce a redshift in the electronic transition of 0.10 eV and 0.13 eV, respectively. This redshift is explained by a more CT-like transition in the chromophore when a water molecule is attached. Theory does not predict the right direction of the shift but does show that the electrostatic interaction between a water molecule and the ion competes with decoupling of acceptor and donor states, which is reflected in both bond lengths and enhanced CT. This is in contrast to the *meta* isomer where the addition of a water molecule hardly changes the coupling, and the electrostatic effect therefore dominates giving a large blueshift (both according to experiment and theory).

Our results have provided important insights into the effects of single water molecules or amino-acid residues (serine or threonine OH groups) on the absorption by biochromophores

containing the phenolate moiety. Next step would be to follow the stepwise effect of attachment of water molecules to ***p***. The first few water molecules likely bind to the negative charge end decoupling donor and acceptor groups and thereby causing gradual redshifts. As water starts to bind at the nitro group, the absorption moves back towards the blue as the coupling between the donor and acceptor groups are reestablished. Future experiments are planned to test this hypothesis but are difficult due to low ion beam currents.

FIGURES

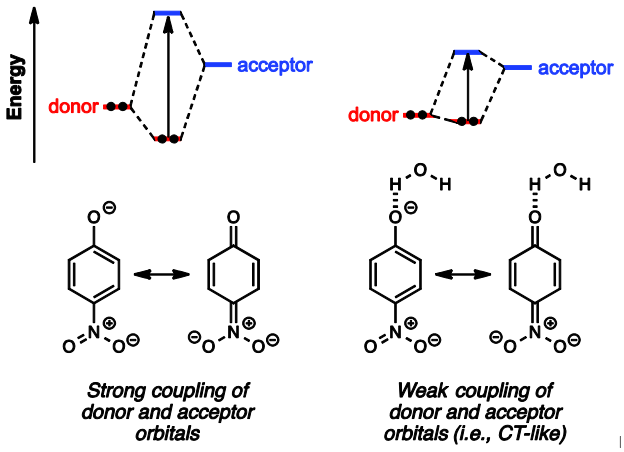

Figure 1. Left: The HOMO and LUMO for *p*-nitrophenolate are linear combinations of orbitals located on a phenolate group (denoted donor) and and a nitro group (acceptor) due to strong coupling (two important resonance forms). The electronic transition is ππ* where the π and π* states are fully delocalized. Right: A single water molecule may decouple the two groups such that the HOMO becomes more donor-like and the LUMO more acceptor-like, simply because the contribution of the resonance form with the electron on the NO_2 group, remotely located from the water, becomes insignificant. The ππ* transition is now CT-like as electron density moves from one end of the molecule to the other.

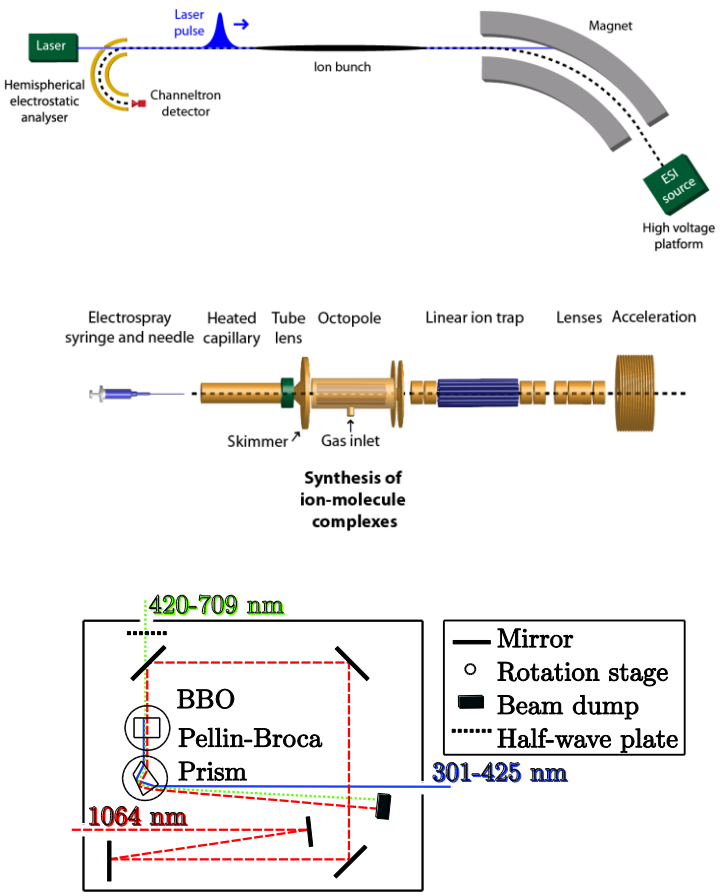

Figure 2. Top: Mass spectrometer setup (see text for details). Middle: The ion source. Water vapor is let into the octopole to produce ion-molecule complexes. Bottom: Illustration of the home-built sum-frequency generator, where IR and visible light are mixed in a BBO crystal to produce UV light. The delay line for the 1064-nm IR beam is for matching in time the visible beam from the OPO. A Pellin-Broca prism is used to separate the two pump beams from the generated beam.

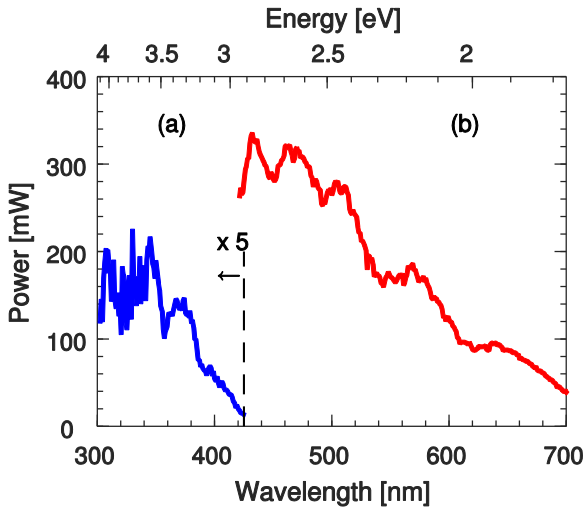

Figure 3. Laser power as a function of output wavelength. (a) Output from sum-frequency generation multiplied by a factor of five. (b) Output from the EKSPLA OPO (visible region). The pulse energy is the power divided by the laser repetition rate (20 s^{-1}).

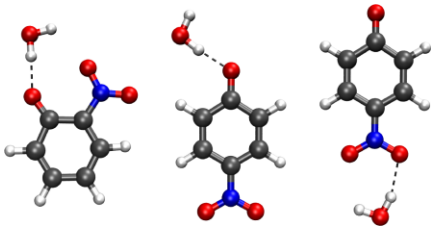

Figure 4. Calculated (PBE0/aug-cc-pVDZ) structures of ***o***·H_2O, ***p***·H_2O@$PheO^-$, and ***p***·H_2O@NO_2.

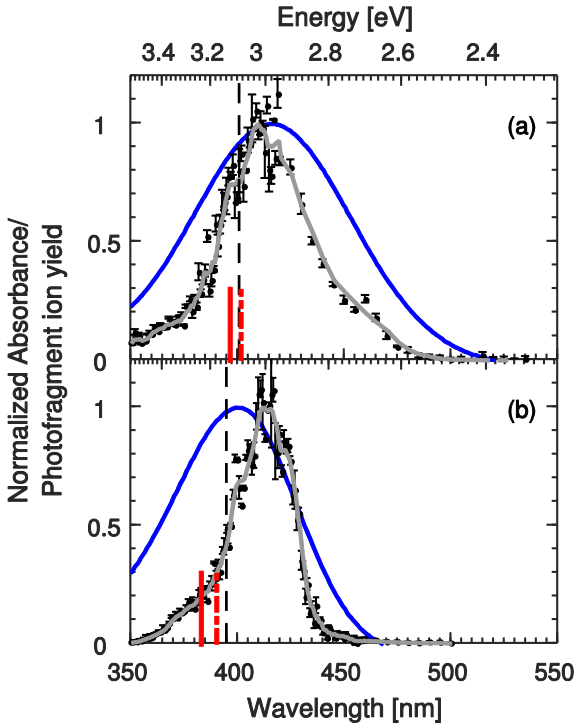

Figure 5. Action spectra of (a) ***o***·H_2O and (b) ***p***·H_2O. To help guide the eyes, a five point average curve (grey) is superimposed on the data. The blue curves are the absorbance spectra obtained in alkaline aqueous solution (pH 10) (the pK_a of both *o*-nitrophenol and *p*-nitrophenol is 7.2). The thick red vertical lines in the bottom of the spectra marks the CC2-calculated band maxima, the full lines are for the water complexes, and the broken lines are for the bare chromophores. The band maxima for the bare chromophores are marked by the broken vertical lines that span the whole height of the figures.

Table 1. Summary of experimental band maxima and calculated vertical excitation energies (in eV).

	Experimental λ_{max}	CC2	ADC(2)	SORCI	NEVPT2
o	3.11	3.15	3.02	3.00	3.24
o·H_2O	3.01	3.20	3.06	3.05	3.29
o$_{(aq)}$	3.00		2.76	2.96	3.16
P	3.16	3.27	3.10	3.11	3.38
p·H_2O	3.00	3.33	3.16	3.23	3.50
p$_{(aq)}$	3.11		2.77	2.98	3.25

Table 2. Calculated bond lengths (Å) and SCS-CC2/aug-cc-pVDZ vertical excitation energies (eV). Difference in dipole moments between excited and ground states, $|\Delta\mu_{10}|$ (D), are given in parentheses. Geometries were optimized with SCS-MP2/aug-cc-pVDZ. Right column: bare solute with the same geometry as in the complex.

	C-O	C-N	Complex	H_2O removed
o	1.265	1.451	3.09 (3.9)	
o·H_2O	1.271	1.452	3.13 (4.1)	3.09 (3.9)
p	1.268	1.425	3.18 (4.8)	
p·H_2O@Phe	1.280	1.434	3.24 (6.1)	3.17 (5.2)
p·H_2O@NO_2	1.264	1.411	3.13 (3.0)	3.21 (4.0)

ASSOCIATED CONTENT

Supporting Information. Calculated geometries and CC2 data using PBE0 geometries are supplied as Supporting Information. This material is available free of charge via the Internet at http://pubs.acs.org.

AUTHOR INFORMATION

Corresponding Author

* E-mail: E-mail: angel.rubio@ehu.es; sbn@hphys.au.dk.

ACKNOWLEDGMENT

SBN acknowledges support from the Danish Council for Independent Research (grant no. 4181-00048B). AR and MW acknowledge financial support from the European Research Council Advanced Grant DYNamo (ERC-2010- AdG-267374), Spanish Grant (FIS2013-46159-C3-1-P), Grupos Consolidados UPV/EHU del Gobierno Vasco (IT578-13). Technical and human support provided by IZO-SGI (SGIker) of UPV/EHU.

ABBREVIATIONS

ADC(2), Algebraic Diagrammatic Construction to 2nd Order; BBO, Barium Borate; BSSE, Basis Set Superposition Error; CC, Coupled Cluster; CT, Charge Transfer; EOM, Equation-of-Motion; GFP, Green Fluorescent Protein; HBDI, 4-HydroxyBenzylidene-2,3-DimethylImidazolinone; HOMO, Highest Occupied Molecular Orbital; IR, Infrared; LUMO, Lowest Unoccupied Molecular Orbital; OPO, Optical Parametric Oscillator; PAH, Polycyclic Aromatic Hydrocarbon; pCA (*para*-Coumaric Acid); PYP, Photoactive Yellow Protein; VEE, Vertical Excitation Energy; ZPVE, Zero Point Vibrational Energy.

REFERENCES

(1) Alata, I.; Dedonder, C.; Broquier, M.; Marceca, E.; Jouvet, C. Role of the Charge-Transfer State in the Electronic Absorption of Protonated Hydrocarbon Molecules. *J. Am. Chem. Soc.* **2010**, *132*, 17483.

(2) Brøndsted Nielsen, S.; Brøndsted Nielsen, M.; Rubio, A. Spectroscopy of Nitrophenolates in Vacuo: Effect of Spacer, Configuration, and Microsolvation on the Charge-Transfer Excitation Energy *Acc. Chem. Res.* **2014**, *47*, 1417.

(3) Alata, I.; Broquier, M.; Dedonder-Lardeux, C.; Jouvet, C.; Kim, M.; Sohn, W. Y.; Kim, S.; Kang, H.; Schütz, M.; Patzer, A.; Dopfer, O. Microhydration effects on the electronic spectra of protonated polycyclic aromatic hydrocarbons: [naphthalene-$(H_2O)_{n=1,2}$]H^+. *J. Chem. Phys.* **2011**, *134*, 074307.

(4) Dopfer, O.; Patzer, A.; Chakraborty, S.; Alata, I.; Omidyan, R.; Broquier, M.; Dedonder, C.; Jouvet, C. Electronic and vibrational spectra of protonated benzaldehyde-water clusters, [BZ-$(H_2O)_{(n<=5)}$] H^+: Evidence for ground-state proton transfer to solvent for n >= 3. *J. Chem. Phys.* **2014**, *140*, 124314.

(5) Niwa, H.; Inouye, S.; Hirano, T.; Matsuno, T.; Kojima, S.; Kubota, M.; Ohashi, M.; Tsuji, F. I. Chemical nature of the light emitter of the Aequorea green fluorescent protein. *Proc. Natl. Acad. Sci. USA* **1996**, *93*, 13617.

(6) Nielsen, S. B.; Lapierre, A.; Andersen, J. U.; Pedersen, U. V.; Tomita, S.; Andersen, L. H. Absorption spectrum of the green fluorescent protein chromophore anion in vacuo. *Phys. Rev. Lett.* **2001**, *87*, 228102.

(7) Sinicropi, A.; Anduniow, T.; Ferre, N.; Basosi, R.; Olivucci, M. Properties of the emitting state of the green fluorescent protein resolved at the CASPT2//CASSCF/CHARMM level. *J. Am. Chem. Soc.* **2005**, *127*, 11534.

(8) Bravaya, K.; Khrenova, M. G.; Grigorenko, B. L.; Nemukhin, A. V.; Krylov, A. I. Effect of Protein Environment on Electronically Excited and Ionized States of the Green Fluorescent Protein Chromophore. *J. Phys. Chem. B* **2011**, *8*, 8296.

(9) Gromov, E. V.; Burghardt, I.; Köppel, H.; Cederbaum, L. S. Electronic structure of the PYP chromophore in its native protein environment. *J. Am. Chem. Soc.* **2007**, *129*, 6798.

(10) Gromov, E. V.; Burghardt, I.; Köppel, H.; Cederbaum, L. S. Native hydrogen bonding network of the photoactive yellow protein (PYP) chromophore: Impact on the electronic structure and photoinduced isomerization. *J. Photochem. Photobiol., A* **2012**, *234*, 123.

(11) de Groot, M.; Gromov, E. V.; Köppel, H.; Buma, W. J. High-resolution spectroscopy of methyl 4-hydroxycinnamate and its hydrogen-bonded water complex. *J. Phys. Chem. B* **2008**, *112*, 4427.

(12) Zuev, D.; Bravaya, K. B.; Makarova, M. V.; Krylov, A. I. Effect of microhydration on the electronic structure of the chromophores of the photoactive yellow and green fluorescent proteins. *J. Chem. Phys.* **2011**, *135*, 194304.

(13) Philip, A.; Eisenman, K.; Papadantonakis, Hoff, W. Functional Tuning of Photoactive Yellow Protein by Active Site Residue 46. *Biochemistry* **2008**, *47*, 13800.

(14) Navizet, I.; Liu, Y. J.; Ferré, N.; Xiao, H. Y.; Fang, W. H. Color-Tuning Mechanism of Firefly Investigated by Multi-Configurational Perturbation Method. *J. Am. Chem. Soc.* **2010**, *132*, 706.

(15) Cai, D.; Marques, M. A. L.; Milne, B. F.; Nogueira, F. Bioheterojunction Effect on Fluorescence Origin and Efficiency Improvement of Firefly Chromophores. *J. Phys. Chem. Lett.* **2010**, *1*, 2781.

(16) Støchkel, K.; Hansen, C. N.; Houmøller, J.; Nielsen, L. M.; Anggara, K.; Linares, M.; Norman, P.; Nogueira, F.; Maltsev, O. V.; Hintermann, L.; Brøndsted Nielsen, S.; Naumov, P.; Milne, B. F. On the Influence of Water on the Electronic Structure of Firefly Oxyluciferin Anions from Absorption Spectroscopy of Bare and Monohydrated Ions in Vacuo. *J. Am. Chem. Soc.* **2013**, *135*, 6485.

(17) Wanko, M.; Houmøller, J.; Støchkel, K.; Kirketerp, M.-B. S.; Petersen, M. Å.; Brøndsted Nielsen, M.; Brøndsted Nielsen, S.; Rubio, A. Substitution effects on the absorption spectra of nitrophenolate isomers. *Phys. Chem. Chem. Phys.* **2012**, *14*, 12905.

(18) Houmøller, J.; Wanko, M.; Støchkel, K.; Rubio, A.; Brøndsted Nielsen, S. On the Effect of a Single Solvent Molecule on the Charge-Transfer Band of a Donor-Acceptor Anion. *J. Am. Chem. Soc.* **2013**, *135*, 6818.

(19) Støchkel, K.; Milne, B. F.; Brøndsted Nielsen, S. Absorption Spectrum of the Firefly Luciferin Anion Isolated in Vacuo. *J. Phys. Chem. A* **2011**, *115*, 2155.

(20) Wyer, J. A.; Brøndsted Nielsen, S. Absorption by Isolated Ferric Heme Nitrosyl Cations In Vacuo. *Angew. Chem., Int. Ed.* **2012**, *51*, 10256.

(21) TURBOMOLE V7.0 2015, a development of University of Karlsruhe and Forschungszentrum Karlsruhe GmbH, 1989-2007, TURBOMOLE GmbH, since 2007.

(22) Christiansen, O.; Koch, H.; Jørgensen, P. The 2nd-Order Approximate Coupled-Cluster Singles and Doubles Model CC2. *Chem. Phys. Lett.* **1995**, *243*, 409.

(23) Schirmer, J. Beyond the Random-Phase Approximation - A New Approximation Scheme for the Polarization Propagator. *Phys. Rev. A* **1982**, *26*, 2395.

(24) Neese, F. A spectroscopy oriented configuration interaction procedure. *J. Chem. Phys.* **2003**, *119*, 9428.

(25) Angeli, C.; Cimiraglia, R.; Evangelisti, S.; Leininger, T.; Malrieu, J. P. Introduction of n-electron valence states for multireference perturbation theory. *J. Chem. Phys.* **2001**, *114*, 10252.

(26) Neese, F. WIREs Comput. Mol. Sci. The ORCA program system. **2012**, *2*, 73.

Table of Contents Graphic

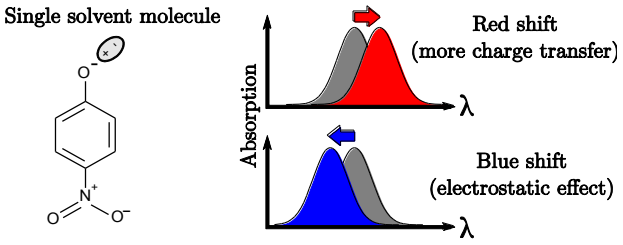

Here we address whether a single water molecule causes the absorption by *o*- and *p*-nitrophenolate to redshift or blueshift.